An Ink Transport Model for Prediction of Feature Size in Dip Pen Nanolithography

Sourabh K. Saha and Martin L. Culpepper*

Laboratory for Manufacturing and Productivity, Department of Mechanical Engineering, Massachusetts Institute of Technology, Cambridge, Massachusetts 02139

Received: June 24, 2010; Revised Manuscript Received: August 2, 2010

Feature size predictions in dip pen nanolithography are typically based upon the constant transport rate or the constant tip−concentration approximations. Models based upon these approximations are inaccurate due to the erroneous assumption that the diffusion of ink upon the surface and ink dissolution at the tip are independent. Herein, we explain that these two steps are related and that they share the same ink flow via the meniscus. We use this insight to generate a comprehensive ink transport model. Our model provides new insight into the (i) relative importance of tip-side transport and surface diffusion, (ii) cause of intermittent line writing at high writing speeds, and (iii) critical role of proper tip inking with respect to feature size accuracy and high-speed writing. We show that the constant rate and constant tip−concentration approaches are limiting cases of the same model, thereby unifying the two approaches and reducing errors in line width prediction by up to 30%.

1. Introduction

Dip pen nanolithography (DPN) is a flexible nanoprocess for creating 2-D patterns.[1–3] In DPN, a sharp, "inked" tip is used to deposit ink molecules directly onto a substrate. Stable patterns are formed on the surface via either chemisorption based self-assembly or physisorption. A schematic of self-assembled monolayer (SAM) formation during the DPN process is provided in Figure 1. Dots are written when a stationary tip is brought into contact with a surface and line features form when a tip travels on the surface. In both cases, concentration-driven diffusion of ink from the tip to the surface leads to the formation of features that are comprised of SAMs. Ink transport from the tip to the surface is mediated by the water meniscus which forms when the tip is brought in contact with the surface.

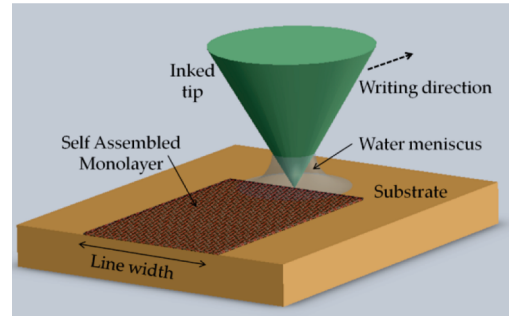

Figure 1. Schematic of dip pen nanolithography line writing process.

DPN has been used to fabricate a variety of devices for biomedical diagnostics, chemical sensors, and nanoelectronics.[4–8] The impact of these devices will only be realized if these devices may be mass manufactured. This in turn requires accurate models of the writing process that enable control of feature size. Process modeling in DPN is often based upon empirical calibration approaches[9] or models with limited scope that account for only one of the relevant ink transport steps.[10–13] What is needed is a comprehensive DPN model that incorporates all ink transport steps as the ink travels from the tip to the surface. Herein we show the relationship among the various transport steps in DPN and use this knowledge to generate a comprehensive model. We use this to (i) show the relative influence of each step on the process and (ii) demonstrate improved accuracy of model predictions relative to experimental results.

Although empirical studies have identified the key parameters that affect feature size in DPN writing,[14,15] they have not clarified *how* changing these parameters changes the ink transport. For example, it is observed that dot diameter and line width increase with an increase in ambient temperature. This is a useful, qualitative "rule of thumb"; however, experiments are not well-suited to uncover whether the effect is due to an increase in tip "strength", or rate of surface diffusion, or some combination that depends upon ink/substrate or other parameters. This type of missing knowledge leads to the need for assumptions and iteration/calibration procedures, which unfortunately fail at some point.

For example, the tip is commonly assumed to be a constant flow rate source. This works well for dot writing[10,16] but fails when writing lines at high speeds. Specifically the assumption is at odds with observations of increased ink transport rate that occurs at high writing speed.[12,17,18] We also note that a constant rate model cannot explain the intermittent writing that is observed at high writing speeds. In summary, the limitations of current DPN line writing models are their inability to accurately predict (i) the relative importance of the parameters and their effect on ink transport and (ii) feature sizes over a wide range of writing speeds.

To a large extent, DPN transport models have focused upon the surface diffusion phenomenon.[10,11] The tip is assumed to be a constant "strength" source and transport is assumed to occur due to 2-D surface diffusion from the tip to the substrate. We have earlier shown that the constant tip−concentration assumption is more accurate than the constant flow rate approach[18] but can be improved upon. The constant tip−concentration approach predicts the increase in flow rate with writing speed but may be improved upon as it overestimates flow rate at higher speeds. This suggests a decrease in concentration with writing speed.

* To whom correspondence should be addressed, culpepper@mit.edu.

10.1021/jp105855n

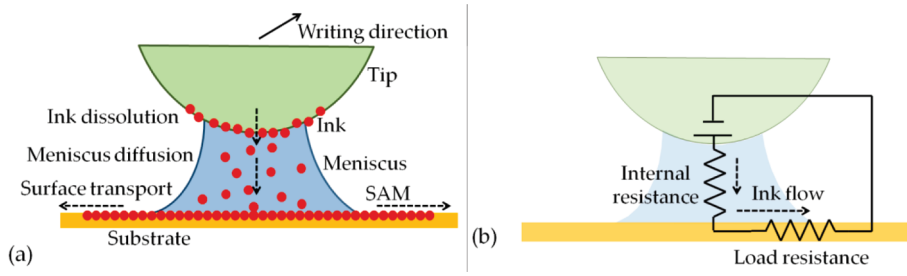

Figure 2. Ink transport in DPN. (a) Cross-sectional view of the tip and the meniscus showing (i) ink dissolution at the tip, (ii) diffusion through the meniscus, and (iii) transport on the surface. (b) Galvanic cell analogy of ink transport in DPN.

Errors associated with models that assume constant rate and constant concentration suggest that the tip: (i) does not act independently from the surface and (ii) cannot be calibrated for constant rate or concentration.

This hypothesis is supported by transport models that describe ink dissolution at the tip and use ink solubility properties to estimate source strength or feature size.[12,13] They do not however link tip-side transport and surface diffusion. Herein, we describe ink dissolution at the tip, diffusion via the meniscus, and surface diffusion as three serial steps that share the same flow of ink. This is used to build a model that (i) accurately predicts line width and (ii) provides a quantitative basis for understanding the influence of key parameters on feature size.

2. Ink Transport in DPN

2.1. Ink Transport Steps. Ink is transported by diffusion from the tip to the surface via a water meniscus that mediates the flow. Figure 2a shows the three steps by which ink transport occurs: (i) dissolution of ink into the meniscus at the tip−meniscus interface, (ii) diffusion via the meniscus to the meniscus−surface interface, and (iii) diffusion from the meniscus−surface interface over the substrate surface.

Compared to previous approaches, this three-step process more accurately represents reality for two reasons. First, the meniscus−surface interface serves as the source for diffusion on the substrate rather than the tip surface. Second, the meniscus affects the flow of ink from the tip to the substrate and this is now captured. The latter is of particular import as the meniscus offers a resistance to ink flow, and as a result the meniscus ink concentration changes with writing speed. We use an analogy to a galvanic cell, as shown in Figure 2b, to explain this behavior. In our analogy (i) ink mass flow is analogous to electrical current, (ii) ink concentration difference across the meniscus and the SAM free surface is analogous to potential difference, (iii) ink concentration on the tip surface is analogous to emf, and (iv) the resistance to diffusion via the meniscus is analogous to the cell's internal resistance. At high writing speeds, ink mass flow (current) increases and this leads to a drop in the ink concentration (potential difference) at the meniscus−surface interface. This occurs because of the resistance to diffusion via the meniscus (internal resistance) even though the ink concentration on the tip surface (emf) remains the same.

2.2. Transport Step Models. A cross-sectional view of the meniscus and the ink flow paths is shown in Figure 3. In this section we explain the following assumptions and use them to construct models for the transport steps: (i) ink dissolution is a first-order chemical reaction, (ii) meniscus geometry may be represented by an equivalent uniform cylinder, (iii) diffusion via the meniscus is one-dimensional with concentration gradient only along the axis of the cylindrical meniscus, and (iv) steady state ink flow occurs during line writing.

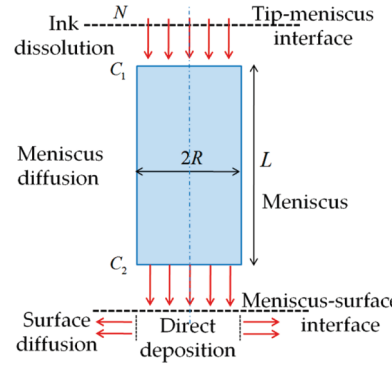

Figure 3. Models of the meniscus and the ink transport steps in DPN line writing that were used for developing the comprehensive model.

Ink Dissolution at the Tip. Ink dissolves from a solid state into the water meniscus at the tip−meniscus interface. We follow Weeks et al.[12] and Giam et al.[13] by modeling this dissolution as a first-order chemical reaction. The rate of forward reaction depends upon the number of ink molecules on the tip, N, and the rate of backward reaction depends upon the volumetric ink concentration at the tip−meniscus interface, C_1. It is possible to estimate the net ink flow rate from the tip, J, in terms of the amount of ink, the ink concentration, and the water solubility properties of the ink. The net ink flow from the tip is therefore

$$J = N\alpha - C_1\beta \tag{1}$$

In eq 1, the first term on the right-hand side is the rate of forward reaction whereas the second term is the rate of backward reaction. The coefficients α and β capture the effect of ink solubility and tip−meniscus geometry. They are calculated via

$$\alpha = \nu e^{-E_d/kT} \tag{2}$$

$$\beta = A\sqrt{\frac{kT}{2\pi m}}e^{-E_a/kT} \tag{3}$$

In eqs 2 and 3, ν is the attempt frequency for ink detachment from tip, E_d and E_a are activation energy for detachment and reattachment, k is Boltzmann constant, T is ambient temperature, A is surface area of the tip in contact with the meniscus, and m is the molecular mass of the ink.

Ink Transport via the Meniscus. Some experimental evidence suggests ink transport *through* the meniscus[15,16] and some that suggests transport *along the periphery* of the meniscus.[11,19] Regardless, the important issue is that the ink on the tip is not in direct contact with the substrate surface and an intermediary

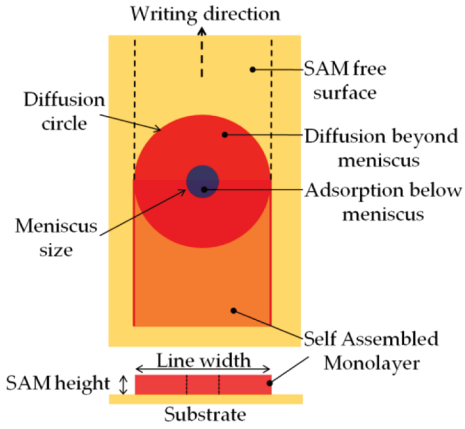

Figure 4. Model of ink transport on the surface during line writing. Ink diffuses out from the meniscus and forms a "diffusion circle" around the tip. As the tip moves, the line is generated as the locus of this circle.

medium exists between the tip and the surface. The water meniscus acts as this medium for hydrophilic inks such as the commonly used alkanethiol 16-mercaptohexadecanoic acid (MHA). We model ink transport via the meniscus as 1-D Fickian diffusion through a uniform cylindrical geometry with only axial ink concentration gradient. We also neglect the meniscus dynamics and consider a stable meniscus. These approximations may seem overly "simple", but it will be shown to be an accurate, elegant means of representing constraints on the ink flow. Therefore, we represent the ink flow rate through the meniscus as

$$J = \frac{D_l(\pi R^2)}{L}(C_1 - C_2) \tag{4}$$

In eq 4, D_l is the ink diffusivity in water, R and L are radius and height of the cylinder that represents the meniscus and C_2 is the volumetric concentration at the meniscus−surface interface.

Transport on the Surface. Transport on the surface may be separated into two components that are depicted in Figures 3 and 4. The first is due to adsorption of ink molecules directly below the meniscus and the second is 2-D surface diffusion of ink molecules beyond the boundaries of the meniscus.

The total flow is a sum of the individual components

$$J = J_1 + J_2 \tag{5}$$

When the tip size is small compared to feature size, as in dot writing, direct adsorption below the meniscus, J_1, is negligible in comparison to the surface diffusion, J_2. During line writing, J_1 may be significant in comparison to J_2 at high writing speeds due to the continuous exposure of the moving tip to the SAM free surface. The direct adsorption flow is related to the tip velocity, V, and surface density of molecules in the SAM, ρ, by

$$J_1 = \rho V(2R) \tag{6}$$

For the 2-D diffusion component, we have generated a model for the surface diffusion phenomenon.[18] Surface diffusion is modeled as a concentration-driven flow of ink with (i) a nonzero ink concentration at the tip and (ii) zero concentration at the line edge boundary. Steady-state ink flow occurs when the line width is uniform along the length. From the tip frame of reference, diffusion in line writing is similar to that in dot writing but with a boundary of constant size. Diffusion from the tip leads to the formation of a "diffusion circle" around the tip, and the line is generated as this diffusion circle moves with the tip. A schematic of the model is shown in Figure 4. This allows us to represent the diffusion component of the flow as

$$J_2 = \frac{2\pi D_s C_0}{\ln(w/2R)} \tag{7}$$

In eq 7, D_s is the ink diffusivity for transport over the SAM layer, C_0 is the surface ink concentration at the meniscus−surface interface, and w is the width of the line. To integrate this diffusion model within the comprehensive model, we note that C_0 depends upon the writing speed, V. We also note that C_0 is related to the volumetric concentration, C_2, and the SAM height, Z_t, by

$$C_0 = Z_t C_2 \tag{8}$$

Mass conservation may be used to link the flow rate to the line width as

$$J = \rho V w \tag{9}$$

Equations 5, 6, 7, 8, and 9 are used in combination to relate line width to ink concentration via

$$\rho V(w - 2R)\ln\frac{w}{2R} = 2\pi D_s Z_t C_2 \tag{10}$$

3. Comprehensive Transport Model

3.1. Model Development. If the ink concentration within the meniscus is known, an estimate of line width and transport rate may be made via eq 10. This is impractical as the ink flow rate, and therefore ink concentration, changes with writing speed. The amount of ink on the tip is independent of writing speed and may therefore be accurately set by controlling the initial tip inking procedure. Given the preceding, it is more useful to relate line width to the amount of ink on the tip instead of relating it to the tip concentration. Here, we represent the meniscus ink concentrations in terms of the amount of ink on the tip. From eqs 1 and 9 we obtain

$$C_1 = \frac{N\alpha - \rho V w}{\beta} \tag{11}$$

We use eqs 4, 9, and 11 and a nondimensional parameter we define as $b = 1 + \beta l/(\pi R^2 D_l L)$ to obtain

$$C_2 = \frac{N\alpha - b\rho V w}{\beta} \tag{12}$$

From eq 12 it is evident that the effective tip concentration for surface diffusion decreases as ink flow rate increases.

Finally, using eq 10 and substituting for C_2 from eq 12, we link line width to the amount of ink on the tip

$$a\rho V(w - 2R)\ln\frac{w}{2R} + b\rho Vw = N\alpha \qquad (13)$$

In eq 13, we use a nondimensional parameter we define as $a = \beta/(2\pi D_s Z_t)$ for brevity. Equation 13 is particularly important as this may be used to ascertain the relative import of the parameters that affect line width. This is best understood if one understands the physical meaning of the terms in eq 13 and how they relate to each other. First we consider which diffusive processes that the parameters a and b represent. Specifically, a scales with the ratio of backward ink flow at the tip to *diffusion on the surface* and b scales with the ratio of backward ink flow to *meniscus diffusion*. As such, the first term on left-hand side represents the effect of the surface diffusion on line width whereas the second term represents the effect of diffusion through the meniscus on line width. The balance between them describes the total ink flow in the forward direction from the tip. This is represented by the term on the right-hand side of eq 13. Equation 13 gives us the ability to (i) compare and contrast the relative ink flows and thereby understand how they affect the process and (ii) control the process by tuning ink flows relative to each other via altering the meniscus, ink, and substrate properties. We will discuss some examples.

While writing with inks that exhibit high surface diffusivity and low meniscus diffusivity ($a \ll b$) the first term in eq 13 effectively "drops out" and the ink flow rate becomes independent of writing speed. This physically represents the case when the surface diffusion is so fast that flow is limited by diffusion through the meniscus. Such an operating regime may be desirable as it simplifies line width predictions via a constant flow rate calibration approach. Similarly, while writing with inks that exhibit high meniscus diffusivity and low surface diffusivity ($b \ll a$), the second term in eq 13 effectively drops out and the ink flow resembles that of constant concentration as given by eq 10. This corresponds to the case when the flow is limited by surface diffusion rather than the meniscus diffusion. A higher flow rate may be supported under a constant concentration condition; therefore this would be a desirable regime for high-speed writing. Our model allows one to determine if an ink satisfies the conditions for a constant flow rate assumption or a constant concentration assumption or if the ink is written via a combination of the two effects.

Our model also explains the phenomenon of intermittent writing that is observed at high writing speeds. It may also be used to predict the "cutoff" speed at which intermittent writing begins. The physical basis for intermittent writing is the limitation on transport rate that manifests from the kinetics of ink dissolution at the tip. As the flow rate increases at high writing speeds, ink concentration at the meniscus−surface interface, C_2, decreases. The cutoff speed corresponds to the writing condition where this concentration effectively drops to zero. Beyond this speed, the steady-state ink transport condition is not valid and the flow exhibits transients that cycle through zero and nonzero values depending on the instantaneous ink concentration in the meniscus. This intermittent flow leads to lengthwise discontinuities in the line pattern. The cutoff writing speed may be estimated by setting C_2 to zero in eq 12 and then using eq 13 to evaluate the corresponding line width as $w = 2R$. Thus, the cutoff speed, V_c, is

$$V_c = \frac{N\alpha}{2Rb\rho} \qquad (14)$$

The import of the model is underscored by the fact that in DPN literature, measured feature sizes and transport rates have been the only physical quantities that enable one to infer the effects of parameters that influence DPN. Equation 14 provides us with a means to use the experimentally measured cutoff speeds to infer DPN characteristics. The cutoff speed depends upon the amount of ink on the tip and the meniscus diffusivity, but it is independent of surface diffusivity. As such, one may use measurements of cutoff speed to study and characterize the effect of control parameters (e.g., ambient temperature and humidity) on tip-side transport in a way that is independent of surface diffusion. Equations 13 and 14 also indicate that control of the tip inking procedure and the meniscus properties are critical for supporting accurate, continuous line writing at high speeds.

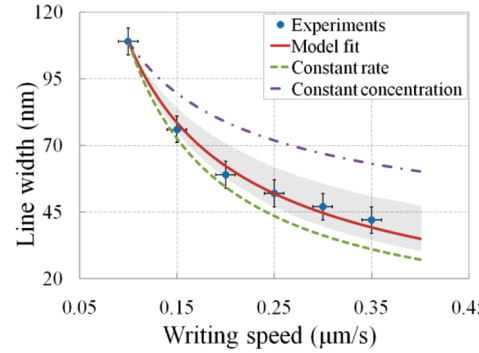

Figure 5. Comparison of model predictions of line width to DPN experiments. Writing was done at an ambient temperature of 298 K and a relative humidity of 33%. Experimental data points in the form V (μm/s), w (nm) are as follows: 0.1, 109; 0.15, 76; 0.2, 59; 0.25, 52; 0.3, 47; and 0.35, 42.

3.2. Model Verification. We performed a set of experiments with MHA ink and evaporated gold-on-silicon substrate (Au(111)) to verify the model. We used this particular combination because it is one of the most commonly used alkanethiol ink systems for DPN writing. As it was not possible to measure the amount of ink on the tip, the right-hand side of eq 13, $N\alpha$, was calibrated by using one data point. Calibration errors due to line width measurement errors were minimized by selecting the point with the lowest writing speed. At this point, the calibrated N is least sensitive to the line width (i.e., $\partial N/\partial w$ is lowest here). From the experimental data in Figure 5 it is clear that line width decreases with increase in the writing speed, which is as expected. In terms of line width predictions, at high writing speeds the constant rate approximation underestimates line width by about 26% whereas the constant concentration approximation overestimates by about 50%.

To verify our model, we first calculated the parameters a and b from the ink properties and meniscus size and then used eq 13 to predict the line widths. We estimated the meniscus radius, $R = 12.5$ nm, via experiments using the measured values of cutoff writing speed and slope of the line width versus writing speed plot. Using eqs 13 and 14, meniscus radius can be related to the slope of width vs speed and the cutoff speed as

$$\frac{\partial w}{\partial V}^{V=V_c} = -\frac{2R}{V_c} \qquad (15)$$

Equation 15 provides a means to estimate the meniscus radius entirely from experiments without requiring any material properties.

The ink solubility parameter, β, was evaluated as 1.16×10^{-16} m^3/s using eq 3, with a surface area $A = \pi R^2$, $m = 4.79 \times 10^{-22}$ g/molecule, and $E_a = 0.13$ eV.[12] Diffusivity in water

TABLE 1: Values of *a* and *b* over the Range of Values of Meniscus Height and Surface Ink Diffusivity

meniscus height, L	surface ink diffusivity, D_s: 5×10^{-9} m^2/s	surface ink diffusivity, D_s: 25×10^{-9} m^2/s
2 nm	$a = 1.84$, $b = 1.54$ (toward constant concentration)	$a = 0.37$, $b = 1.54$
10 nm	$a = 1.84$, $b = 3.68$	$a = 0.37$, $b = 3.68$ (toward constant rate)

meniscus, $D_l = 8.78 \times 10^{-10}$ m^2/s, was evaluated using the Einstein−Stokes relationship.[20] The meniscus height, L, and ink diffusivity on SAM, D_s, were not accurately known; therefore their values were bounded within a range (see section S1 in Supporting Information). Their upper and lower limits along with the corresponding values of a and b are shown in Table 1. With this range of a and b, the predicted line width lies within the shaded region of Figure 5. This region is smaller than the one bounded by the constant rate and constant concentration curves and corresponds to a worst case prediction error of 18% on the constant rate side and 22% on the constant concentration side.

From a least-squares error fit of the model to the experiments, we found that $L = 5$ nm and $D_s = 1.37 \times 10^{-8}$ m^2/s. With these values we obtained the calibrated total flow, $N\alpha = 1.6 \times 10^5$ molecules/s, and calculated $a = 0.66$ and $b = 2.34$. The flow $N\alpha$ represents an upper limit to the net ink flow and is close to the reported DPN ink flow values of $(0.7-4) \times 10^5$ molecules/s.[10,13] The comparable magnitudes of a and b indicate that both surface diffusion and diffusion through the meniscus are significant. The higher value of b as compared to a suggests that the second term in eq 13 is dominant and therefore surface diffusion is faster than meniscus diffusion. The higher b value also explains why in this case the constant rate approximation is more accurate than the constant concentration approximation.

Our best fit model predicted a cutoff writing speed of 0.57 μm/s. We ran a set of experiments to verify this cutoff speed. First, we wrote a set of lines over a wide range of writing speeds from 0.01 to 5 μm/s. We observed that the cutoff lies within 0.25 and 1 μm/s, as is shown in Figure 6a. We used the force profiles along the length of the line to distinguish between the continuous and discontinuous lines (see section S2 in Supporting Information). Next, we wrote a set of lines within the range of 0.25−1 μm/s. As shown in Figure 6b, we observed that the cutoff speed lies within 0.44 and 0.63 μm/s, which is consistent with the model prediction. Further division of the 0.44−0.63 μm/s range was not done because at this range it was not possible to reliably distinguish the discontinuous lines from the continuous lines.

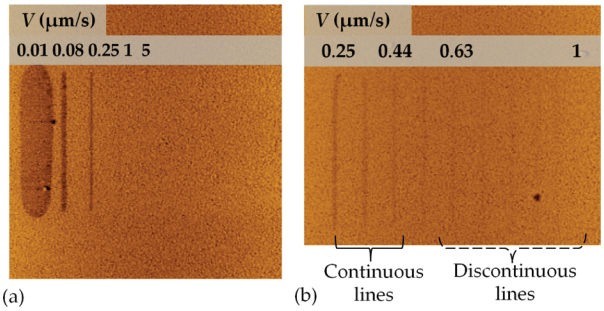

Figure 6. Lateral force microscopy scans of lines that were written to identify the cutoff writing speed. (a) Lines were written with writing speed in the range of 0.01−5 μm/s. (b) From left to right, writing was done at 0.25, 0.34, 0.44, 0.53, 0.63, 0.72, 0.81, 0.91, and 1 μm/s. Discontinuous lines were observed beyond 0.44 μm/s.

The amount of ink on the tip reduces with continuous writing and this may cause a concern that a constant one-time calibrated N value would not capture the changes in the amount of ink on the tip during writing, thereby leading to inaccurate model predictions. To check this, we calculate the change in the amount of ink during writing and compare this to the initial inking. From the calibrated $N\alpha$ value we find that for an estimated α of 10^{-3} (see section S3 in Supporting Information), $N \sim 10^8$ molecules, whereas the loss in N after writing a line 100 nm wide and 3 μm long is $\Delta N \sim 10^6$ molecules, suggesting ~1% decrease in N. This corresponds to an error of ~1% in the line width prediction of eq 13. Therefore, for practical purposes the change in the amount of ink during writing may be neglected for short lines. Here "short" depends upon the required accuracy. If one desires excellent width control when writing over large areas with the same tip, it may be necessary to modify the model so that it accounts for the drop in the amount of ink during writing.

3.3. Model in Perspective. We have developed a simplified ink transport model that accounts for all of the steps, thereby unifying the constant rate and constant concentration approaches within the same model. However, our approximations with respect to the meniscus may seem to be overly "simple". There may be a concern that the *idealized* model parameters do not correspond to the *realistic* conditions due to (i) noncylindrical geometry of a real meniscus or (ii) the role of meniscus in ink transport for hydrophobic inks. To deal with this, we separate out the relevant meniscus properties that independently influence the three transport steps and then identify the means to relate the model parameters to the real meniscus properties. Thus, when the real meniscus geometry is known, one can "map" its properties to the model parameters.

For the ink dissolution step, we have approximated the tip−meniscus interface area in eq 3 by the area at the top of the cylindrical meniscus. For a real meniscus, one can use the meniscus and tip geometry to evaluate the actual surface area of the tip in contact with the meniscus. This affects the parameters N and β by changing the amount of ink available for transport on the tip and the cross section for backward ink flow. For the meniscus diffusion step, the effect of meniscus on ink transport is quantified by the resistance to ink flow, i.e., through the term $D_l(\pi R^2)/L$ in eq 4. For a real meniscus, this idealized resistance should be replaced by the equivalent flow resistance of the meniscus as obtained from its geometry. Finally, the effect of meniscus on the surface diffusion step is through the meniscus footprint radius, i.e., the explicit R terms in eqs 10 and 13. For a real meniscus, this footprint radius may not be the same as the radius of the meniscus at the tip−meniscus interface. Although one may use the real meniscus geometry to predict the footprint, it can also be experimentally measured by using eq 15. This set of "mapping" techniques also works for hydrophobic inks or inks that do not diffuse *through* the meniscus. Our model can be applied to such inks by indentifying (i) the area of tip surface that has ink available for transport, (ii) ink flow resistance of the medium between the tip and surface, and (iii) the tip footprint radius for surface diffusion.

Our model relates line width to the parameters that directly affect ink transport. However, for practical purposes, process control in DPN is often carried out via control of the ambient conditions, i.e., by controlling the ambient temperature and the relative humidity. Effect of these parameters on line width is implicit in our model through (i) temperature-dependent material properties and (ii) temperature and humidity dependent meniscus geometry. The effect of the former can be accounted for by using temperature-dependent properties as is done in eqs 2 and

3. However, one needs to model the meniscus geometry to quantify the effect of the latter. Nevertheless, a qualitative estimate of the effect of changes in the meniscus geometry can be obtained by separately considering the three steps. Meniscus size increases with an increase in the relative humidity and a decrease in the ambient temperature. This leads to (i) an increase in the area of the tip−meniscus interface, (ii) decrease in the meniscus flow resistance, and (iii) an increase in the tip footprint radius. Thus, the net effect is an increase in the ink transport rate and the line width. This is consistent with experimental observations of the effect of temperature and humidity on DPN writing with MHA ink.[14,15]

4. Conclusions

We have developed a model for DPN line writing that improves the line width prediction accuracy as compared to the constant rate and constant concentration approximations. More importantly, our model accounts for the relevant steps involved in transport of ink from the tip to the surface. This has allowed us to separate out, and individually quantify, the effects of the tip, meniscus, and surface on line width. We are also able to ascertain the relative import and effect of each step on the process. We were thereby able to identify the relevant tip, meniscus and ink properties that directly affect line width in DPN. Thus, our transport model provides a powerful framework that may be used to analyze and engineer the DPN process. For example (i) by suitably tuning the meniscus and ink properties one may achieve writing conditions that correspond to a constant rate or a constant concentration condition and (ii) the phenomenon of intermittent writing at high speeds may be explained and predicted using transport rate limitation considerations.

We also show that calibrating a tip for the amount of ink on the tip provides a more accurate line width prediction as opposed to calibrating the tip for constant rate or concentration. Thus, control of the tip inking process, as opposed to simply "dipping" the tip in the ink solution, is critical for improving the accuracy of feature size prediction and process control. Although a few precise tip inking procedures have been experimentally demonstrated,[21,22] their impact upon accurate feature generation is not apparent in the context of our model. Our model provides a theoretical framework, based upon ink transport, that shows the need for precise inking and analyzing its effect on feature generation. This model also lays the groundwork for model refinements. For example, new insights from the use of noncylindrical water meniscus geometries and a 3-D meniscus diffusion model.

Acknowledgment. We thank the Pappalardo graduate fellowship fund for supporting this work and thank NanoInk for access to, and permission to use, their DPN 5000 system in our research. This material is based in part upon work supported by the National Science Foundation under Grant No. 0914790—" Center for Affordable Nanoengineering of Polymeric Biomedical Devices (CANPBD)".

Supporting Information Available: Selecting the range of values for meniscus height and surface ink diffusivity, empirical estimation of cutoff writing speed, and estimation procedure for ink solubility parameter α. This information is available free of charge via the Internet at http://pubs.acs.org.

References and Notes

(1) Piner, R. D.; Zhu, J.; Xu, F.; Hong, S.; Mirkin, C. A. *Science* **1999**, *283*, 661–663.
(2) Haaheim, J.; Nafday, O. A. *Scanning* **2008**, *30*, 137–150.
(3) Ginger, D. S.; Zhang, H.; Mirkin, C. A. *Angew. Chem., Int. Ed.* **2004**, *43*, 30–45.
(4) Lim, J.-H.; Ginger, D. S.; Lee, K.-B.; Heo, J.; Nam, J.-M.; Mirkin, C. A. *Angew. Chem., Int. Ed.* **2003**, *42*, 2309–2312.
(5) Su, M.; Li, S.; Dravid, V. P. *J. Am. Chem. Soc.* **2003**, *125*, 9930–9931.
(6) Chung, S.-W.; Ginger, D. S.; Morales, M. W.; Zhang, Z.; Chandrasekhar, V.; Ratner, M. A.; Mirkin, C. A. *Small* **2005**, *1*, 64–69.
(7) Hung, S.-C.; Nafday, O. A.; Haaheim, J. R.; Ren, F.; Chi, G. C.; Pearton, S. J. *J. Phys. Chem. C* **2010**, *114*, 9672–9677.
(8) Salaita, K.; Wang, Y.; Mirkin, C. A. *Nat. Nanotechnol.* **2007**, *2*, 145–155.
(9) Haaheim, J.; Eby, R.; Nelson, M.; Fragala, J.; Rosner, B.; Zhang, H.; Athas, G. *Ultramicroscopy* **2005**, *103*, 117–132.
(10) Jang, J.; Hong, S.; Schatz, G. C.; Ratner, M. A. *J. Chem. Phys.* **2001**, *115*, 2721–2729.
(11) Nafday, O. A.; Vaughn, M. W.; Weeks, B. L. *J. Chem. Phys.* **2006**, *125*, 144703–4.
(12) Weeks, B. L.; Noy, A.; Miller, A. E.; De Yoreo, J. J. *Phys. Rev. Lett.* **2002**, *88*, 255505.
(13) Giam, L. R.; Wang, Y.; Mirkin, C. A. *J. Phys. Chem. A* **2009**, *113*, 3779–3782.
(14) Rozhok, S.; Piner, R.; Mirkin, C. A. *J. Phys. Chem. B* **2002**, *107*, 751–757.
(15) Peterson, E. J.; Weeks, B. L.; De Yoreo, J. J.; Schwartz, P. V. *J. Phys. Chem. B* **2004**, *108*, 15206–15210.
(16) Huang, L.; Chang, Y.-H.; Kakkassery, J. J.; Mirkin, C. A. *J. Phys. Chem. B* **2006**, *110*, 20756–20758.
(17) Schwartz, P. V. *Langmuir* **2002**, *18*, 4041–4046.
(18) Saha, S. K.; Culpepper, M. L. *Appl. Phys. Lett.* **2010**, *96*, 243105–3.
(19) Sheehan, P. E.; Whitman, L. J. *Phys. Rev. Lett.* **2002**, *88*, 156104.
(20) With a MHA footprint of 0.229 nm^2, effective molecule size $r =$ 0.27 nm and with water dynamic viscosity $\mu = 9 \times 10^{-4}$ N s/m^2 at $T =$ 298 K, ink diffusivity in water was evaluated using the Einstein−Stokes relationship as: $D_l = kT/(6\pi\mu r)$.
(21) Rosner, B.; Duenas, T.; Banerjee, D.; Shile, R.; Amro, N.; Rendlen, J. *Smart Mater. Struct.* **2006**, *15* (1), S124.
(22) Wang, Y.; Giam, L. R.; Park, M.; Lenhert, S.; Fuchs, H.; Mirkin, C. A. *Small* **2008**, *4*, 1666–1670.

JP105855N